Laser Physics Letters

Astro Ltd.

LETTER

Entanglement improvement of entangled coherent state via multiphoton catalysis

To cite this article: Weidong Zhou *et al* 2018 *Laser Phys. Lett.* **15** 065203

IOP Publishing | Astro Ltd
Laser Physics Letters
Laser Phys. Lett. **15** (2018) 065203 (12pp)
https://doi.org/10.1088/1612-202X/aaba4f

Letter

Entanglement improvement of entangled coherent state via multiphoton catalysis

Weidong Zhou[1], Wei Ye[1], Cunjin Liu[1], Liyun Hu[1] and Sanqiu Liu[1,2]

[1] Center for Quantum Science and Technology, Jiangxi Normal University, Nanchang 330022, People's Republic of China
[2] Department of physics, Nanchang University, Nanchang 330031, People's Republic of China

E-mail: huliyun@jxnu.edu.cn and sqlgroup@ncu.edu.cn

Received 5 March 2018, revised 27 March 2018
Accepted for publication 27 March 2018
Published 4 May 2018

Abstract

Based on the conditional measurement and beam splitters, multi-photon catalysis is introduced to each mode of even entangled coherent states (EECSs). The resulted states belong to a kind of Laguerre polynomials excited EECSs. Then the entanglement properties of resulted state are examined according to EPR correlation, concurrence and the teleportation fidelity. For the symmetrical beam splitters, these three quantities can be improved by multi-photon catalysis ($\geqslant$3) and only EPR correlation can be enhanced by zero-photon catalysis. Our optimal results over transmissivities of beam splitters show that the unit concurrence can be achieved for all non-zero photon catalysis which indicates that the optimized output approaches Bell-type state. In addition, two single-photon catalysis and zero-photon catalysis present better performance for the improvement of both the EPR correlation and the teleportation fidelity in small and large amplitude regions, respectively. Particularly, it is interesting to notice that both of them can be optimized to be constant for zero-photon catalysis when the amplitude exceeds a certain threshold.

Keywords: quantum ctatlysis, quantum entanglement, entangled coherent states

(Some figures may appear in colour only in the online journal)

1. Introduction

Quantum entanglement, as a kind of key resource, has been widely applied in quantum communication and quantum information processing [1–3]. In order to realize effectively a long distance quantum communication, it is generally necessary to produce different entangled states which are expected to be robust to decoherence from the environments. Thus, it maybe an alternative way to prepare high entanglement quantum states experimentally. However, the actually available resources are featured with a finite degree of entanglement due to the experimental limitation. To obtain high entanglement and complete long distance quantum tasks, many researchers turn attention to local non-Gaussian operations, including photon subtraction, photon addition and the polynomial operation combination of both. It is shown that it is possible to accomplish the improvement of entanglement and nonclassical properties as well as quantum teleportation fidelity [4–20]. In addition, these non-Gaussian operations also play important role in other fields, such as quantum tomography [21], quantum metrology [22] and quantum cryptography [23–25].

As the superpositions of multimode coherent states, entangled coherent states (ECSs) have attracted widespread interest in many fields [26–34]. For example, an improved phase estimation can be achieved by employing ECSs, which outperforms other popular two-mode entangled states [27, 28]. One can refer [35] about a review of ECSs. On the other hand, the generalization beyond the ECSs is also interesting. For instance, photon-added coherent states and two-mode

photon-added even entangled coherent states (EECSs) are proposed by operating directly photon-creation operator [36, 37]. Single-photon-added coherent state is also applied to the quantum key distribution and shows great advantage compared to all other existing sources [38]. In addition, the superposition of photon-creation and photon-annihilation operators has been acted on each mode of the EECSs [13]. It is shown that the EPR correlation can be improved in a small region of amplitude (about <0.52) and the improvement effects by coherent superposition operation are more prominent than those by single or two-photon addition in a certain region of amplitude. These results suggest that non-Gaussian operations including photon-addition, photon-subtraction and the superposition of both can be used to enhance the non-classical properties including the entanglement degree and the teleportation fidelity.

Different from these non-Gaussian operators mentioned above, quantum-optical catalysis without photon-added or photon-subtracted was also proposed to generate nonclassical states and enhance the entanglement of quantum system [39–41]. For example, the quantum-optical single-photon catalysis experimentally realized the effect of undoing loss on quantum entanglement [42]. In addition, two-mode catalysis has also been used to distill the entanglement of two-mode squeezed state. In particular, a better performance is achieved by symmetrical single-photon catalysis case than other cases [43]. Recently, the process has been further extended to the case consisting of nonlinear parametric down-conversion and conditional measurement [19]. A theoretical protocol is produced for generating Laguerre polynomial excited coherent states by exploiting two-mode squeezing transformation and conditional measurement with coherent states as input. It is shown that the produced output state presents obvious nonclassical properties which can be modulated by coherent amplitude, squeezing parameter and measured photon-number.

As a natural generalization beyond the ECSs, in this paper, we shall apply multiphoton catalysis on each mode of the EECSs and focus on the entanglement enhancement for a clear understanding the effects of the quantum catalysis. It should be noted that the multiphoton catalysis requires conditional measurements with the resolution of single photon level, which has been overcome by time-multiplexed detectors [9]. In addition, the catalysis operator with EECSs input can be used to generate Laguerre polynomial excited EECSs (LPE-EECSs) $|\Psi\rangle_{out}$ (see equation (6) below). The paper is organized as follows. In section 2, we introduce the multiphoton catalysis scheme and derive analytical expression of the input-output relation for single mode catalysis. Then we operate the operation on each mode of the EECSs and derive the normalization factor which is found to be related to the two-variable Hermite polynomials. In section 3, we investigate the entanglement properties of the LPE-EECSs by means of the EPR correlation and the concurrence. In section 4, we further examine the fidelity of teleportation by using the LPE-EECSs as entangled channel. Our primary results are summarized in the last section.

2. Theoretical model by heralded interference

2.1. Theoretical model

As shown in figure 1 we present a scheme for generating an optical state $|\psi\rangle_{out}$ with the assistance of heralded interference and multiphoton catalysis. This system consists of two modes labeled as a and b. In mode a, an m-photon Fock state $|m\rangle$ is firstly fed to the input port, and then is incident on the beam splitter with the transmissivity $T_1 = \cos^2\theta$. An arbitrary quantum state is incident on the other input port denoted as mode b. Subsequently, a photon-number projective measurement is performed at one of the output mode. The quantum-optical process is called as multiphoton catalysis. When an arbitrary state denoted as $|\varphi\rangle_{in}$ is injected into the input port of mode b, the generated optical state $|\Psi\rangle_{out}$ by the catalysis process can be given by

$$|\psi\rangle_{out} = N_m \, {}_a\langle m| B(T_1) |m\rangle_a |\varphi\rangle_{in}, \tag{1}$$

where N_m is the normalization constant, and $B(T_1) = e^{\theta(a^\dagger b - a b^\dagger)}$ is the beam splitter operator with $T_1 = \cos^2\theta$. It is a primary task to work out the matrix element $\hat{O}_m \equiv {}_a\langle m| B(T_1) |m\rangle_a$. For this purpose, using the normal ordering form of $B(T_1)$ [44, 45], i.e.

$$\begin{aligned} B(T_1) =: \exp\{&\left(\sqrt{T_1} - 1\right)\left(a^\dagger a + b^\dagger b\right) \\ &+ \left(a^\dagger b - a b^\dagger\right)\sqrt{R_1}\} :, \end{aligned} \tag{2}$$

where $R_1 = 1 - T_1$ is the reflectivity, and the coherent state representation of Fock state

$$|m\rangle = \frac{1}{\sqrt{m!}} \frac{\partial^m}{\partial \alpha^m} |\,|\alpha\rangle\,|_{\alpha=0}, \; |\,|\alpha\rangle = e^{\alpha a^\dagger} |0\rangle\,|_{\alpha=0}, \tag{3}$$

the operator $\hat{O}_m$ can be then calculated as

$$\begin{aligned} \hat{O}_m =:& H_{m,m}\left(-\frac{b^\dagger\sqrt{R_1}}{i\sqrt{T_1}}, \frac{b\sqrt{R_1}}{i\sqrt{T_1 T_1}}\right) : \\ &\times \frac{\left(-\sqrt{T_1}\right)^m}{m!} e^{b^\dagger b T \ln T_1/2} \\ =& T_1^{m/2} : L_m\left(b^\dagger b R_1/T_1\right) : e^{b^\dagger b \ln T_1/2}, \end{aligned} \tag{4}$$

where $L_m(.)$ is the Laguerre polynomials and $H_{m,m}(x, y)$ is the two-variable Hermite polynomials connected by the following the relation $(-1)^m H_{m,m}(x, y)/m! = L_m(xy)$. Additionally, we here employed the operator identity $: e^{\left(e^\lambda - 1\right) b^\dagger b} : \; = e^{\lambda b^\dagger b}$, and $e^{\lambda b^\dagger b} b e^{-\lambda b^\dagger b} = e^{-\lambda} b$. From equation (4), when $m = 0$, it is ready to get $\hat{O}_0 = e^{b^\dagger b \ln T_1/2}$; while for $m = 1$, we see $\hat{O}_1 = \left(1 - b^\dagger b R_1/T_1\right) e^{b^\dagger b \ln T_1/2} T_1^{1/2}$. On the other hand, it is clearly seen from equations (1) and (4) that we can construct the relation between the input state and the generated optical state, namely $|\psi\rangle_{out} \to \hat{O}_m |\varphi\rangle_{in}$ which is convenient for further investigating some properties of the generated states in the following sections.

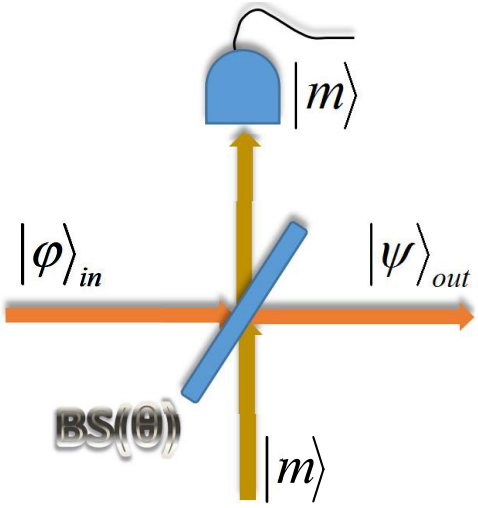

Figure 1. Schematic diagram showing the generation of a new state $|\Psi\rangle_{out}$ by using multiphoton catalysis with a pure state $|\varphi\rangle_{in}$ input (mode b).

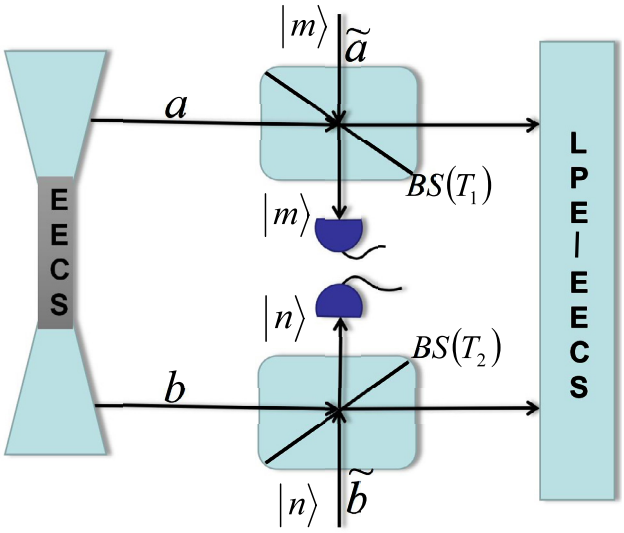

Figure 2. When the input state $|\varphi\rangle_{in}$ is a two-mode EECS, the output state $|\Psi\rangle_{out}$ becomes a new kind of Laguerre polynomial excited even entangled coherent states (LPE-EECSs).

2.2. Even-entangled coherent states as inputs

Among entangled states, the ECSs have the simplest mathematical structure and present many applications in the fields of quantum information and quantum computation [26–35]. On one hand, the preparation of ECSs with large coherent amplitude is very difficult experimentally. On the other hand, when the ECSs are embedded in dissipative channel, it is shown that the larger the initial coherent amplitude is, the faster the entanglement decreases [46]. Thus the ECSs with small coherent amplitude present better performance than those with large one in this sense. It is an interesting question that how to realize the concentration of non-maximally ECSs in a small region of coherent amplitude at current technology level. Actually, in order to realize different tasks, one may construct many different kinds of ECSs [46]. Note that the EECSs can be generated by beam splitter with coherent state and Schrödinger cat state, thus here we only take the EECSs as an example (denoted as $|EECSs\rangle$) and examine the entanglement properties of the catalyzed state. Our method can be generalized to other ECSs case. The EECSs is given by

$$|EECS\rangle = N_z\left(|z\rangle_a \otimes |z\rangle_b + |-z\rangle_a \otimes |-z\rangle_b\right), \tag{5}$$

where $N_z^{-2} = 2[1+e^{-4|z|^2}]$ is the normalization constant. Applying the multiphoton catalysis on each mode of the EECSs shown in figure 2, the final output state is given by

$$|\Psi\rangle_{out} = N_{m,n}\hat{O}_m\hat{O}_n|EECS\rangle, \tag{6}$$

where $N_{m,n}$ is the normalization constant, and the two catalysis operators are defined as $\hat{O}_m \equiv T_1^{m/2}: L_m\left(a^\dagger a R_1/T_1\right): e^{a^\dagger a \ln T_1/2}$ and $\hat{O}_n \equiv T_2^{n/2}: L_n\left(b^\dagger b R_2/T_2\right): e^{b^\dagger b \ln T_2/2}$. In order to clearly show the properties of the outputs, we need to derive some matrix elements such as $A_1 = \langle z|_a \hat{O}_m^\dagger \hat{O}_m |z\rangle_a$. Following the method used in [40], we can obtain

$$\begin{aligned}\hat{O}_m|z\rangle_a &= T_1^{m/2}: L_m\left(a^\dagger a R_1/T_1\right): e^{a^\dagger a \ln T_1/2}|z\rangle_a \\ &= e^{-\frac{1}{2}|z|^2 R_1} T_1^{m/2}: L_m\left(a^\dagger a R_1/T_1\right): \left|z\sqrt{T_1}\right\rangle_a \\ &= e^{-\frac{1}{2}|z|^2 R_1} T_1^{m/2} L_m\left(\mu_m a^\dagger\right)\left|z\sqrt{T_1}\right\rangle_a \\ &= \bar{N}_m L_m\left(\mu_m a^\dagger\right)\left|z\sqrt{T_1}\right\rangle_a,\end{aligned} \tag{7}$$

where $\mu_m = zR_1/\sqrt{T_1}$, $\bar{N}_m = e^{-R_1|z|^2/2}T_1^{m/2}$ and we have used the formula $g^{b^\dagger b}|\alpha\rangle = e^{\left(g^2-1\right)|\alpha|^2/2}|g\alpha\rangle$. It is clear to see that the effects of the operator $\hat{O}_m$ is to reduce the initial amplitude z with a coefficient $\sqrt{T_1}$ and to excite the inputs by the Laguerre polynomials operation. The case is true for the mode b. Thus, equation (6) can be further rewritten as

$$\begin{aligned}|\Psi\rangle_{out} = \bar{N}_{m,n}\{&L_m\left(\mu_m a^\dagger\right)L_n\left(\mu_n b^\dagger\right)|z_1\rangle_a|z_2\rangle_b \\ &+L_m\left(-\mu_m a^\dagger\right)L_n\left(-\mu_n b^\dagger\right)|-z_1\rangle_a|-z_2\rangle_b\},\end{aligned} \tag{8}$$

where $z_j = z\sqrt{T_j}(j=1,2)$, $\bar{N}_{m,n} = N_{m,n}\bar{N}_m\bar{N}_n$ is the normalization factor, and $\mu_n = zR_2/\sqrt{T_2}$ with T_2 being the transmissivity of beam splitter BS(T_2). From equation (8) it is seen that the generated state is just Laguerre polynomial excited EECSs (LPE-EECSs). Particularly, when $T_1 = T_2 = 1$, noticing that $\mu_m = \mu_n = 0$ then equation (8) reduces to equation (5), as expected. While for the case of both $m = n = 0$ and $T = T_1 = T_2$, equation (8) becomes $|\Psi\rangle_{out} = N_{0,0}\{|\gamma\rangle_a|\gamma\rangle_b + |-\gamma\rangle_a|-\gamma\rangle_b\}$ with $\gamma = z\sqrt{T}$. It is shown that, the zero-photon catalysis case can be used to realize the noiseless attenuation [19, 40].

Next, in order to discuss the entanglement properties of the LPE-EECSs in the following sections, it is necessary to derive the explicit expression of $N_{m,n}$, which is

$$N_{m,n}^{-2} = 2\left(A_1B_1 + A_2B_2\right), \tag{9}$$

where the explicit forms of A_1, A_2, B_1 and B_2 are expressed by

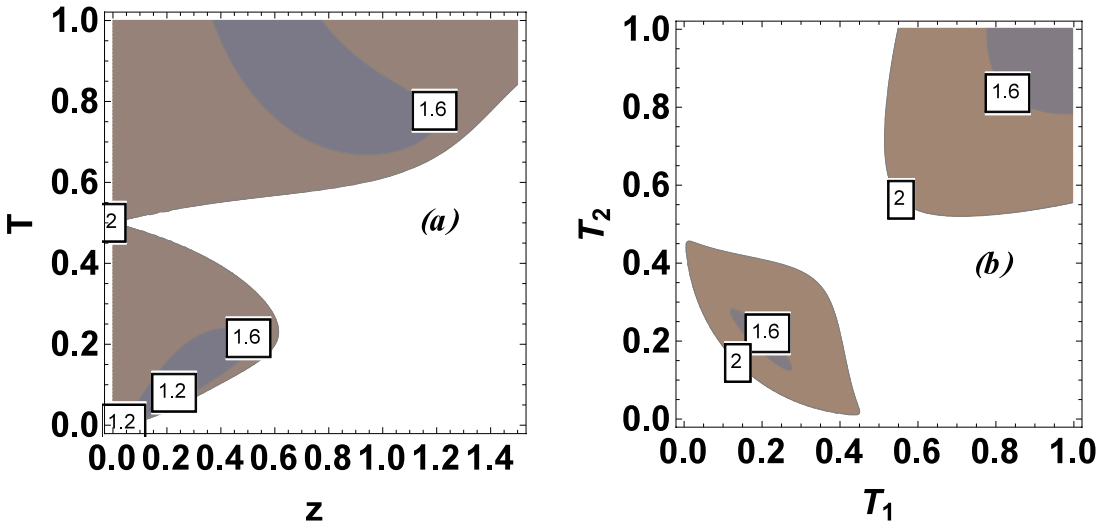

Figure 3. The performance of the EPR correlation of the LPE-EECSs for the single-photon catalysis case, namely, $m = n = 1$, (a): in (z, T) space with $T = T_1 = T_2$, and (b): in (T_1, T_2) space with the amplitude $z = 0.5$. The shading regions correspond to the region with $I < 2$.

$$A_1 = \bar{N}_m^2 \sum_{l,k=0}^{m} \binom{m}{l} \binom{m}{k} \frac{(-\mu_m)^k \mu_m^{*l}}{l!k!} \times H_{k,l}\left(z^* \sqrt{T_1}, -z\sqrt{T_1}\right), \tag{10}$$

$$A_2 = \bar{N}_m^2 \sum_{l,k=0}^{m} \binom{m}{l} \binom{m}{k} \frac{\mu_m^k \mu_m^{*l}}{l!k!} \times e^{-2|z|^2 T_1} H_{k,l}\left(z^* \sqrt{T_1}, z\sqrt{T_1}\right), \tag{11}$$

and B_1 and B_2 can be obtained from A_1 and A_2, respectively, by replacing m and T_1 with n and T_2. In particular, when $m = n = 0$, according to equations (9)–(11), the normalization constant is easily calculated as $N_{0,0}^{-2} = 2e^{-(2+T_1+T_2)|z|^2}[1 + e^{2(T_1+T_2)|z|^2}]$. Moreover, when $T_1 = T_2 = 1$, it is obvious that $N_{0,0}^{-2} = 2[1 + e^{-4|z|^2}] = N_z^{-2}$, which indicates that the LPE-EECSs just reduce to the initial EECSs.

Additionally, before discussing the entanglement properties of the LPE-EECSs in the next section, we here introduce two applicable matrix elements, i.e, $\langle a^q a^{\dagger p}\rangle$ and $\langle b^q b^{\dagger p}\rangle$, whose analytical expressions are, respectively, given by

$$\begin{aligned} \langle a^q a^{\dagger p}\rangle &= N_{m,n}^2 \left[\left(O_{A_1} + O_{A_4}\right) B_1 + \left(O_{A_2} + O_{A_3}\right) B_2\right], \\ \langle b^q b^{\dagger p}\rangle &= N_{m,n}^2 \left[\left(O_{B_1} + O_{B_4}\right) A_1 + \left(O_{B_2} + O_{B_3}\right) A_2\right], \end{aligned} \tag{12}$$

where A_1 and A_2 have been defined in equation (11), and

$$O_{A1} = \bar{N}_m^2 \sum_{l,k=0}^{m} \binom{m}{l} \binom{m}{k} \frac{(-1)^{q+k} \mu_m^k \mu_m^{*l}}{l!k!} \times H_{k+p,l+q}\left(z^* \sqrt{T_1}, -z\sqrt{T_1}\right), \tag{13}$$

$$O_{A_2} = \bar{N}_m^2 \sum_{l,k=0}^{m} \binom{m}{l} \binom{m}{k} \frac{(-1)^q \left(\mu_m\right)^k \mu_m^{*l}}{l!k!} \times e^{-2|z|^2 T_1} H_{k+p,l+q}\left(z^* \sqrt{T_1}, z\sqrt{T_1}\right), \tag{14}$$

and O_{A_3} and O_{A_4} can be given from O_{A_2} and O_{A1} by replacing q with p, respectively. The analytical expressions of O_{B_1}, O_{B_2} and O_{B_3}, O_{B_4} can be obtained from O_{A_1}, O_{A_2} and O_{A_3}, O_{A_4} by replacing m and T_1 with n and T_2, respectively, not shown here for simplicity.

3. The entanglement properties of the LPE-EECSs

Actually, many theoretical and experimental schemes have been proposed to improve the properties of entanglement. Hence, in this section, we will examine how the entanglement improvement of the LPE-EECSs is affected by several different photon catalysis numbers and transmissivity. In our scheme, in order to clearly examine the entanglement properties, the methods of the EPR correlation and the concurrence shall be used.

3.1. The EPR correlation

It is well known that the EPR correlation plays an important role in taking account of the inseparability of a bipartite state with continuous-variable, and its definition is expressed as $I = \Delta^2\left(Q_a - Q_b\right) + \Delta^2\left(P_a + P_b\right)$ with I being the total variance of a pair of EPR-type operators, $Q_j = \left(j + j^\dagger\right)/\sqrt{2}$ and $P_j = \left(j - j^\dagger\right)/\left(i\sqrt{2}\right)$, $(j = a \text{ or } b)$. According to equation (8), for the LPE-EECSs, we find that $\langle a\rangle = \langle b^\dagger\rangle = 0$, and thus I can be simplified as

$$I = 2\left\langle aa^\dagger - a^\dagger b^\dagger - ab + bb^\dagger\right\rangle - 2. \tag{15}$$

In order to obtain the explicit expression of the EPR correlation of the LPE-EECSs, here we need to calculate three matrix elements $\langle aa^\dagger\rangle$, $\langle bb^\dagger\rangle$ and $\langle ab\rangle$. Actually, both $\langle aa^\dagger\rangle$ and $\langle bb^\dagger\rangle$ can be directly given by equation (12) by taking $p = q = 1$, i.e.

$$\left\langle aa^{\dagger}\right\rangle = 2N_{m,n}^{2}\left(O_{A_1}B_1 + O_{A_2}B_2\right),$$
$$\left\langle bb^{\dagger}\right\rangle = 2N_{m,n}^{2}\left(O_{B_1}A_1 + O_{B_2}A_2\right). \quad (16)$$

In a similar way, $\langle ab\rangle = \left\langle a^{\dagger}b^{\dagger}\right\rangle^{*}$ can be calculated as

$$\langle ab\rangle = 2N_{m,n}^{2}\left[R_{A1}R_{B1} + R_{A2}R_{B2}\right], \quad (17)$$

where R_{A1} and R_{A2} are defined by

$$R_{A1} = \bar{N}_m^2 \sum_{l,k=0}^{m} \binom{m}{l}\binom{m}{k} \frac{(-1)^{1+k}\mu_m^k \mu_m^{*l}}{l!k!} \times H_{k,l+1}\left(z^*\sqrt{T_1}, -z\sqrt{T_1}\right),$$
$$R_{A2} = \bar{N}_m^2 \sum_{l,k=0}^{m} \binom{m}{l}\binom{m}{k} \frac{\left(\mu_m^*\right)^l \mu_m^k}{l!k!} \times e^{-2|z|^2T_1} H_{k,l+1}\left(z^*\sqrt{T_1}, z\sqrt{T_1}\right), \quad (18)$$

and R_{B1} and R_{B2} can be obtained from R_{A1} and R_{A2}, respectively, by replacing m and T_1 with n and T_2. Particularly, when $m = n = 0$ and $T = T_1 = T_2$, it is not difficult from equations (8) and (15) to get the expression of the EPR correlation with zero-photon catalysis as

$$I_{00} = 2\{2\left|\gamma\right|^2 \tanh(2\left|\gamma\right|^2) - 2\left|\gamma\right|^2\cos\phi + 1\},$$
$$\gamma = \left|\gamma\right| e^{i\phi}. \quad (19)$$

Theoretically, substituting equations (16) and (17) into the equation (15), we can obtain the explicit expression of the EPR correlation of the LPE-EECSs. Particularly, for the limit case of $T_1 = T_2 = 1$, and according to equation (15), the expression of the EPR correlation of the EECSs reads as $I_0 = 2\{2\left|z\right|^2\tanh(2\left|z\right|^2) - 2\left|z\right|^2\cos(2\varphi) + 1\} < 2$ where $z = \left|z\right|\exp(i\varphi)$, as expected. If the total variance of a quantum state is smaller than 2, then it indicates that this quantum state is inseparable or entangled [5, 47]. As shown in figure 3, for the single photon catalysis with $m = n = 1$, we plot the contour map for the EPR correlation function of the LPE-EECSs in (z, T) space with $T = T_1 = T_2$ and in (T_1, T_2) space with the amplitude $z = 0.5$. Here for simplicity we have taken z to be real number in all numerical calculations. From figure 3 it is clearly seen that there are not regions of $I < 2$ which means that the LPE-EECSs are inseparable and the EPR correlation presents a symmetry about T_1 and T_2 (see figure 3(b)). In addition, for a small region of coherent amplitude, there are two regions for $I < 2$ characteristic of $0 < T < 0.5$ and $0.5 < T < 1.0$ (see figure 3(a)); while for a big coherent amplitude, the region of I <2 can be found for a high transmission case.

It is interesting to notice that for the symmetrical beam splitters with $T_1 = T_2 = 0.5$, the region of I <2 with $m = n = 1$ is absent for all coherent amplitude (see figure 3(a)). In order to see this point clearly, we show the EPR correlation as a function of the amplitude z for several different values of $m = n = 0, 1, 2, 3, 4$, as shown in figure 4. From figure 4, it is shown that (i) for the case of $m = n = 1$, the regions of I <2 are absent; while for the case of $m = n = 2, 3, 4$, the regions of I <2 can be found when the amplitude is small; (ii) for zero-photon catalysis case, it is interesting to notice that the

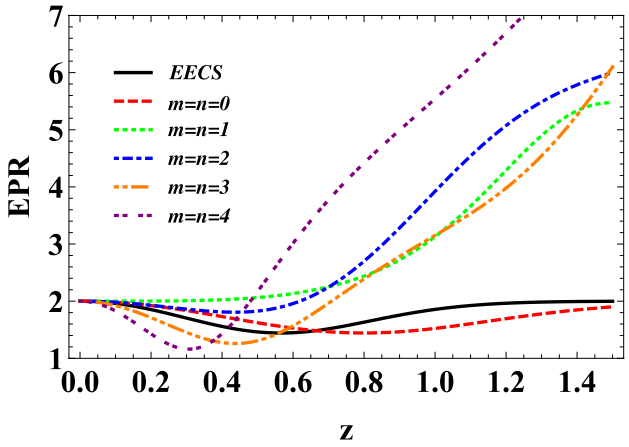

Figure 4. The performance of the EPR correlation of the LPE-EECSs as a function of the amplitude z for the symmetrical beam splitters $T_1 = T_2 = 0.5$ with several different photon catalysis cases $m = n = 0, 1, 2, 3, 4$. Here, for a comparison, we also plot the EPR correlation of the EECSs.

region of $\Delta I = I - I_0 < 0$ can be present in a large amplitude range (about $z > 0.67$). This indicates that zero-photon catalysis can be used to enhance the EPR correlation for the case of large coherent amplitude. Actually, this point can be clear by reviewing equation (19), which has the same form as the EPR correlation of the EECSs except for a smaller amplitude $z\sqrt{T}$ compared to z. Thus for the symmetrical case, one can realize the enhancement of the EPR correlation in small and big amplitude regions by multi-photon catalysis and zero-photon catalysis, respectively.

Generally speaking, the output states $\left|\Psi\right\rangle_{out}$ in equation (8) can be modulated by the transmissivity. For this purpose, we further consider the EPR correlation of the LPE-EECSs in figure 5 by optimizing I to be its minimum over two transmissivity T_1 and T_2 for given coherent amplitude. Here we only examine the two-mode symmetrical photon-catalysis cases with $m = n = 0, 1, 2, 3$. For a comparison, the EPR correlation of the EECSs is also plotted as a function of the amplitude z. From figure 5 it is shown that (i) For the case of zero-photon catalysis with $m = n = 0$, when the amplitude z is less than a threshold value about $z_0 = 0.56$, both the LPE-EECSs and the EECSs share the same EPR correlation. In fact, the case can be understood by optimizing $T_1 = T_2 = 1$ which implies that the output states and the initial states are the same. In another word, there is no enhancement for the EPR correlation in the region of $0 \leqslant z \leqslant z_0$. However, an obvious enhancement of the EPR correlation can be obtained and kept a constant in the large amplitude region of $z_0 < z$. The reason is that the amplitude $\gamma = z\sqrt{T}$ can always equal z_0, i.e. $z\sqrt{T} = z_0$ for the case of $z_0 < z$ by modulating T. (ii) In addition, for given small amplitude range with $z < z_0$, the enhanced region of the EPR correlation becomes smaller as the increasing $m = n = 1, 2, 3$, corresponding to $0 \sim 0.47$ and $0 \sim 0.27$ as well as $0 \sim 0.17$, respectively; while for the large amplitude with $z > z_0$, the cases of $m = n = 1, 2, 3$ share the same enhanced EPR correlation which shows a stronger correlation in initial large amplitude compared to the initial EECSs. The

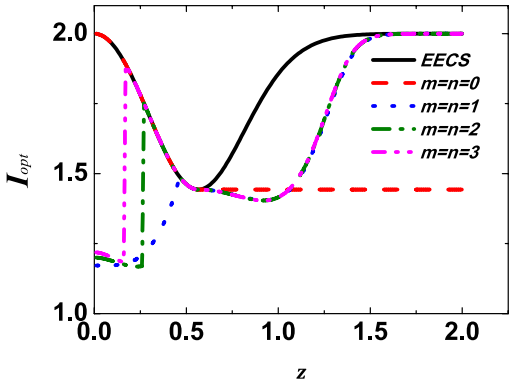

Figure 5. The optimized EPR correlation (denoted by I_{opt})for the LPE-EECSs as a function of the amplitude z with several different photon catalysis cases $m = n = 0, 1, 2, 3$. Here for a comparison, we also plot the EPR correlation of the EECSs.

same values of EPR correlation are shared by both the output states companied by $m = n = 1, 2, 3$ and the initial EECSs as the increasing amplitude ($1.563 \leqslant z$). Thus, two single-photon catalysis presents a better performance for enhancing the EPR correlation in a larger amplitude region compared to that for $m = n = 2, 3$. In addition, the optimal values for $m = n = 1, 2, 3$ exceed that for zero-photon catalysis within a certain amplitude region ($0.56 < z < 1.06$). Thus, single-photon catalysis presents best performance in the region of $0.27 < z < 1.06$, while the zero photon catalysis has same performance in the region of $1.06 < z$ compared to both the EECSs and the LPE-EECSs with $m = n = 1, 2, 3$.

3.2. The concurrence

In this subsection, we will study that how the multiphoton catalysis operating on each mode of the EECSs affects the entanglement of the LPE-EECSs. Here we shall use the concurrence as the measurement. For discrete-variable entangled states like equation (8), the concurrence is an appropriate tool for measuring the degree of quantum entanglement. Referred to [48–50], one can suppose a general bipartite entangled state in the following form

$$|\Psi\rangle = N\left[\mu\,|\eta\rangle_a \otimes |\gamma\rangle_b + \nu\,|\xi\rangle_a \otimes |\delta\rangle_b\right], \tag{20}$$

where $|\eta\rangle_a$ and $|\xi\rangle_a$($|\gamma\rangle_b$ and $|\delta\rangle_b$) are normalized states of subsystem a (subsystem b) with complex numbers μ and ν, and the normalization constant is given by $N^{-2} = |\mu|^2 + |\nu|^2 + 2\,\mathrm{Re}\,(\mu^*\nu P_1 P_2^*)$ in which $P_1 = \langle\eta\,|\xi\rangle_a$, and $P_2 = \langle\delta\,|\gamma\rangle_b$. Thus, using the Schmidt decomposition, the concurrence can be calculated as

$$C = \frac{2\,|\mu|\,|\nu|\left[\left(1-|P_1|^2\right)\left(1-|P_2|^2\right)\right]^{1/2}}{|\mu|^2 + |\nu|^2 + 2\,\mathrm{Re}\,(\mu^*\nu P_1 P_2^*)}. \tag{21}$$

Under the condition $\mu = \pm\nu$, equation (21) reduces to

$$C_{\pm} = \frac{\sqrt{\left(1-|P_1|^2\right)\left(1-|P_2|^2\right)}}{1 \pm \mathrm{Re}\,(P_1 P_2^*)}, \tag{22}$$

which only depends on the overlaps $\langle\eta|\,\xi\rangle_a$ and $\langle\delta|\,\gamma\rangle_b$.

In order to obtain the amount of entanglement of the states via the concurrence, we first introduce the following normalized states:

$$\begin{aligned}
|\pm z\rangle_m &= A_1^{-1/2}\hat{O}_m\,|\pm z\rangle_a \\
&= A_1^{-1/2}T_1^{m/2}{:}\,L_m\left(a^\dagger a R_1/T_1\right){:} \\
&\quad\times e^{a^\dagger a \ln T_1/2}\,|\pm z\rangle_a, \\
|\pm z\rangle_n &= B_1^{-1/2}\hat{O}_n\,|\pm z\rangle_b \\
&= B_1^{-1/2}T_2^{n/2}{:}\,L_n\left(b^\dagger b R_2/T_2\right){:} \\
&\quad\times e^{b^\dagger b \ln T_2/2}\,|\pm z\rangle_b,
\end{aligned} \tag{23}$$

where A_1 and B_1 are defined in equation (10). Then, using four normalized states the final states $|\Psi\rangle_{out}$ can be reconstructed as

$$|\Psi\rangle_{out} = N_{m,n}\left(A_1 B_1\right)^{1/2}\left(|z\rangle_m\,|z\rangle_n + |-z\rangle_m\,|-z\rangle_n\right). \tag{24}$$

Thus, according to equation (20), one can find

$$\begin{aligned}
P_1 &= {}_m\langle z|\,-z\rangle_m = \frac{A_2}{A_1}, \\
P_2 &= {}_n\langle -z\,|z\rangle_n = \frac{B_2}{B_1}.
\end{aligned} \tag{25}$$

By substituting equations (25) into (22), the concurrence of the LPE-EECSs can be given by

$$C = \frac{\sqrt{\left(A_1^2 - A_2^2\right)\left(B_1^2 - B_2^2\right)}}{A_1 B_1 + A_2 B_2}. \tag{26}$$

In particular, for the case of $T_1 = T_2 = 1$, according to equations (26), (10) and (11), it is easy to obtain the concurrence of the EECSs, i.e. $C(EECSs) = (1 - e^{-4|z|^2})/(1 + e^{-4|z|^2})$, as expected. In addition, for the zero-photon catalysis with $m = n = 0$, the concurrence can be easily calculated as

$$C_{00} = \frac{\sqrt{(e^{4T_2|z|^2} - 1)(e^{4T_1|z|^2} - 1)}}{1 + e^{2(T_1+T_2)|z|^2}}, \tag{27}$$

which depends on these two transmissivities, and reduces to the concurrence of the EECSs when $T_1 = T_2 = 1$. When $m = n = 1$ the entanglement is present in four regions: low T_1 and low T_2, high T_1 and high T_2, high T_1 and low T_2 as well as low T_1 and high T_2 (see figure 6(b)). This case is different from the EPR correlation which has only two symmetrical regions of correlation, i.e. low T_1 and low T_2, high T_1 and high T_2 (see figure 3). In this sense, the EPR correlation is more strict than the entanglement for describing quantum correlation. In addition, it is clear seen from figure 6 with given $m = n = 1$ that, for any coherent amplitude z, the concurrence can reach the maximum by choosing $T_1 = T_2 = T$ (see figure 6(a)); while for a given amplitude $z = 0.5$, the concurrence first increases, and then decreases as the increasing $T_1 = T_2 = T$, i.e. there is a peak (see figure 6(b)) which indicates that the concurrence has one chance to be maximized by changing T. We further consider the effects of different parameters T_1, T_2, $m = n$ and z on the concurrence in the following.

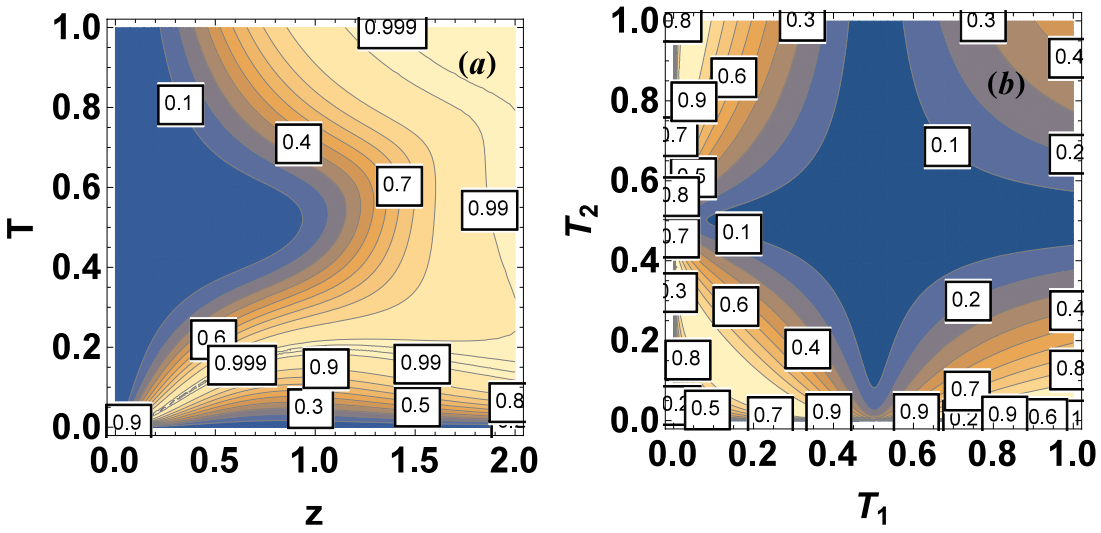

Figure 6. The concurrence of the LPE-EECSs for the single-photon catalysis case, namely, $m = n = 1$, (a): in (z, T) space with $T = T_1 = T_2$, and (b): in (T_1, T_2) space with the amplitude $z = 0.5$.

For symmetrical beam splitters i.e. $T_1 = T_2 = 0.5$, we plot the concurrence as a function of the amplitude z with $m = n = 0, 1, 2, 3, 4$ in figure 7. It is clearly seen that (i) for the catalysis with $m = n = 0, 1, 2$, the concurrence decreases compared to that of the EECSs; especially for zero-photon catalysis, this point can be clear by reviewing equation (8) with a smaller amplitude $z/\sqrt{2}$. (ii) the enhancement of the concurrence can be found for multi-photon catalysis cases (say $m = n = 3, 4$). Specially speaking, the enhanced regions are located at $z \leqslant 1.27$ and $z \leqslant 0.75$ for $m = n = 3, 4$, respectively. (iii) As the catalyzed-photon number increases, the effect becomes better for improving the concurrence in a certain small amplitude region (say $z \lesssim 0.62$). These results show that for symmetrical beam splitter the improved concurrence can only be achieved by multiphoton catalysis over photon-number 3.

Now, we further consider the effect of different transmissivities on the concurrence. For this purpose, we optimize the concurrence over T_1 and T_2 for given amplitude and several different values of $m = n = 0, 1, 2, 3$ in figure 8. It is shown that (i) the optimal results with $m = n = 0$ share the same concurrence as the initial EECSs, which actually corresponds to the full transmission, as expected; (ii) while for non-zero photon catalysis, the output states keep the maximum entanglement by modulating the transmissivity. This indicates that the optimized state approaches Bell-type state, such as $(|00\rangle + |11\rangle)/\sqrt{2}$ which is the maximum entangled state. In order to see this point clearly, we take $T_1 = T_2 = T$ and plot the concurrence as the function of T for several different values of z and $m = n$ in figure 9. It is clearly shown that for given z and $m = n$, the maximum concurrence can be obtained via modulating symmetrical transmissivity T. There are one, two, and three chances for realizing the maximum concurrence for $m = n = 1, 2, 3$, respectively. Specially speaking, for $z = 0.5$ and $m = n = 1, 2$, the T corresponding to maximum concurrence equal to about 0.13, and 0.02 and 0.29. Thus one may prepare approximately the Bell-type state via quantum catalysis and the EECSs.

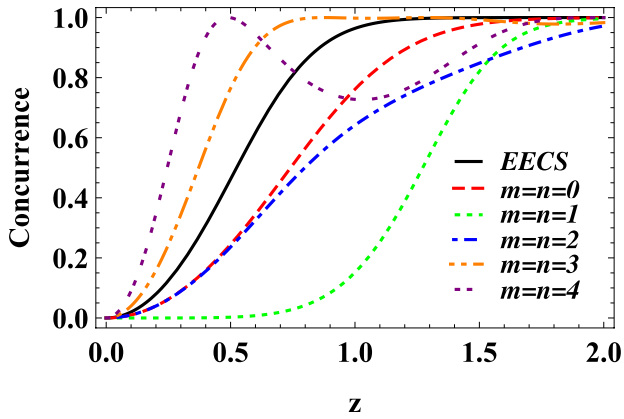

Figure 7. The concurrence of the LPE-EECSs as a function of the amplitude z for the symmetrical beam splitters $T_1 = T_2 = 0.5$ with several different photon catalysis cases $m = n = 0, 1, 2, 3, 4$. Here, for a comparison, the concurrence of the EECSs is also plotted.

4. Fidelity of quantum teleportation

In this section, we investigate the performance of the fidelity of the standard Braunstein–Kimble (BK) protocol to teleport unknown coherent states by using the final states as entangled resource [51, 52]. The approach of [53] pointed out that using the formalism of the characteristic function (CF) is convenient and computational strategies to analyze the fidelity of quantum teleportation. For a two-mode system ρ, the CF is defined as $\chi(\eta, \gamma) = \mathtt{tr}\left[D_a(\eta) D_b(\gamma) \rho\right]$, where D_a, D_b are the displacement operators. Considering the antinormal production form of the displacement operator: $D_a(\eta) = e^{\frac{1}{2}|\eta|^2} e^{-\eta^* a} e^{\eta a^\dagger}$ and $D_b(\gamma) = e^{\frac{1}{2}|\gamma|^2} e^{-\gamma^* b} e^{\gamma b^\dagger}$, the CF of the LPE-EECSs can be calculated as

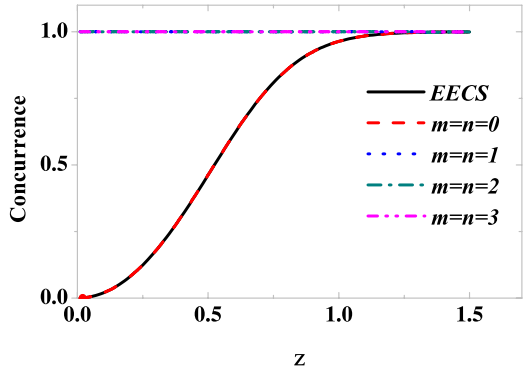

Figure 8. The optimized concurrence of the LPE-EECSs as a function of the amplitude z for several different photon catalysis cases $m = n = 0, 1, 2, 3$. Here for a comparison, we also plot the concurrence of the EECSs.

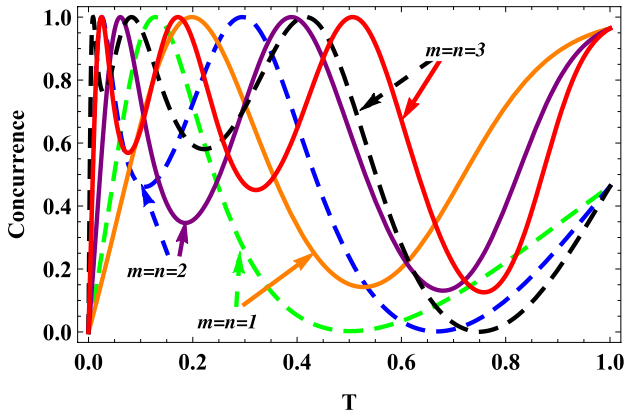

Figure 9. The concurrence of the LPE-EECSs for several different photon catalysis cases $m = n = 1, 2, 3$ as a function of the transmissivity T with $T = T_1 = T_2$ at fixed the amplitude $z = 0.5$ (dashed line) and $z = 1.0$ (solid line).

$$\chi(\eta,\gamma) = N_{m,n}^2 \left\{ \chi^{z,z}(\eta,\gamma) + \chi^{z,-z}(\eta,\gamma) + \chi^{-z,z}(\eta,\gamma) + \chi^{-z,-z}(\eta,\gamma) \right\}, \tag{28}$$

where we have defined $\chi^{\alpha,\beta}(\eta,\gamma) = CF_A^{\alpha,\beta}(\eta)\, CF_B^{\alpha,\beta}(\gamma)$, $(\alpha, \beta = z \text{ or } -z)$, and $CF_A^{\alpha,\beta}(\eta) \equiv {}_a\langle\alpha|\hat{O}_m^\dagger D_a(\eta)\hat{O}_m|\beta\rangle_a$. In order to obtain the explicit form of $CF_A^{\alpha,\beta}(\eta)$, by using equation (7) and the sum representation of Laguerre polynomials, $L_m(x) = \sum_{k=0}^m \binom{m}{k} \frac{(-1)^k}{k!} x^k$, we finally obtain

$$CF_A^{\alpha,\beta}(\eta) = \bar{N}_m^2 e^{-|\eta|^2/2 + (\alpha^*\eta - \eta^*\beta)\sqrt{T_1}} \left\langle \alpha\sqrt{T_1} \middle| \beta\sqrt{T_1} \right\rangle \times \sum_{l,k=0}^{m} \binom{m}{l}\binom{m}{k} \frac{\bar{\mu}_m^k (-\bar{\mu}_m^*)^l}{l!k!} \times H_{k,l}\left[\eta^* - \alpha^*\sqrt{T_1}, \eta + \beta\sqrt{T_1}\right], \tag{29}$$

where $H_{k,l}$ is the two-variable Hermite polynomials, and we have defined $\bar{\mu}_m = \beta R_1/\sqrt{T_1}$ and $\bar{\mu}_m^* = \alpha^* R_1/\sqrt{T_1}$. $CF_B^{\alpha,\beta}(\gamma)$ can be obtained from $CF_A^{\alpha,\beta}(\eta)$ by replacing m, $T_1(R_1)$ and η with n, $T_2(R_2)$ and γ, respectively.

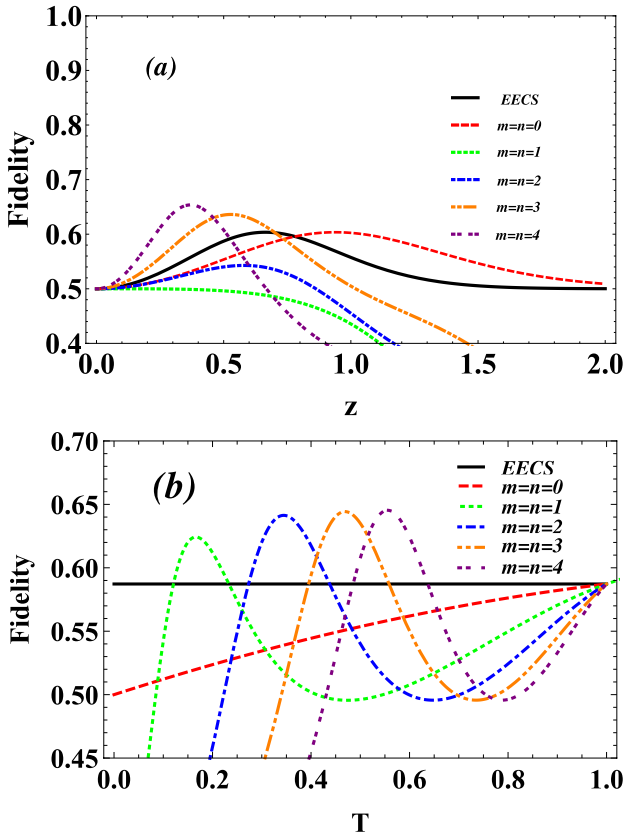

Figure 10. The fidelity of the LPE-EECSs for several different photon catalysis cases $m = n = 0, 1, 2, 3$, and 4, (a) as a function of the amplitude z with the symmetrical beam splitters $T_1 = T_2 = 0.5$. (b) that of the transmissivity T with $T = T_1 = T_2$ at fixed the amplitude $z = 0.5$. Here, for a comparison, we also plot the fidelity of the EECSs.

To obtain the fidelity of teleportation by using the LPE-EECSs as the entangled resource, we return to the following fidelity formula [43, 53], i.e.

$$F = \int \frac{d^2\xi}{\pi} \chi_{in}(\xi)\, \chi_{out}(-\xi), \tag{30}$$

where $\chi_{in}(\xi)$ and $\chi_{out}(-\xi)$ are the CFs of input state ρ_{in} and output state ρ_{out}, respectively. For the ideal BK protocol, the CF of output states (teleported states) is related with the CFs of the input states and the entangled states by the relation $\chi_{out}(\xi) = \chi_{in}(\xi)\, \chi_E(\xi^*, \xi)$ [43, 53], in which $\chi_E(\xi^*, \xi)$ denotes the CF of the entangled resource. In addition, the fidelity is independent of the amplitude of coherent state, thus here for simplicity we only consider the vacuum state as an input state whose CF is given by $\chi_{in}(\xi) = e^{-|\xi|^2}$.

Substituting equations (28) into (30), the fidelity of the LPE-EECSs can be eventually expressed as

$$F = N_{m,n}^2 \left\{ F^{z,z} + F^{z,-z} \right\}, \tag{31}$$

where $F^{\alpha,\beta}$ $(\alpha, \beta = z \text{ or } -z)$ are derived as

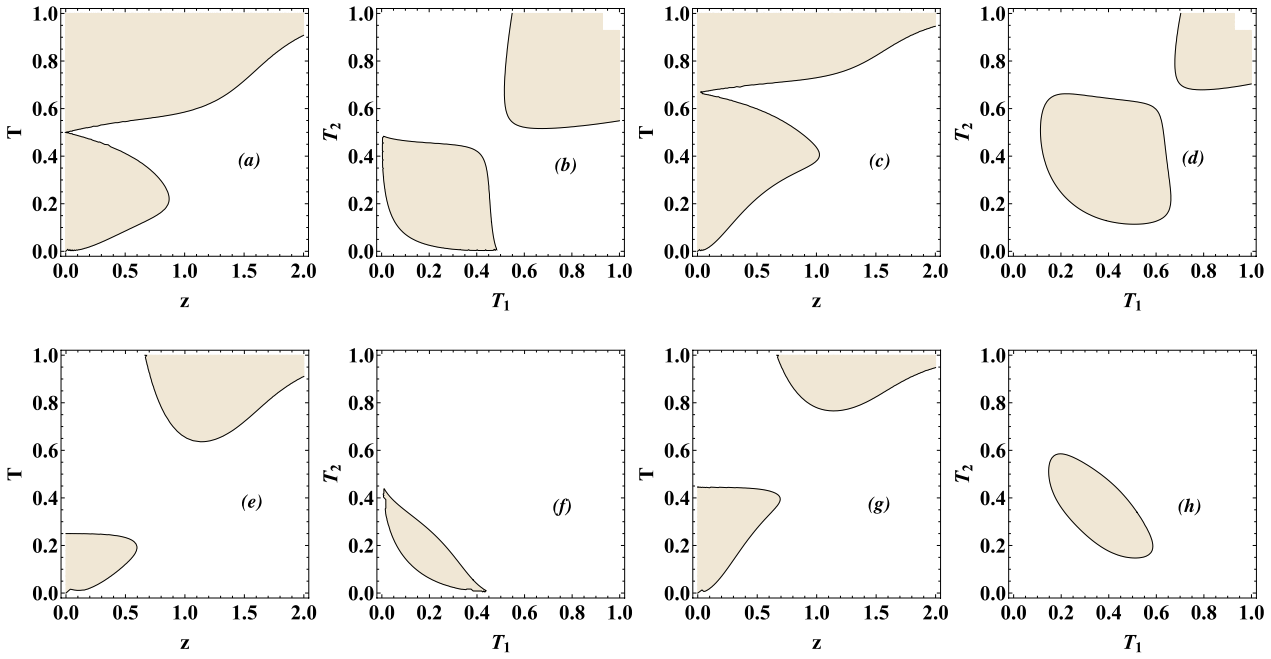

Figure 11. The counterplots of the fidelity for the LPE-EECSs. The first and second row corresponds to $F \geqslant 0.5$ and $\Delta F \geqslant 0$, respectively. The left two columns, and right two columns correspond to $m = n = 1$ and 2, respectively.

$$
\begin{aligned}
F^{\alpha,\beta} &= \int \frac{d^2\xi}{\pi} e^{-|\xi|^2} \chi^{\alpha,\beta}\left(-\xi^*, -\xi\right) \\
&= A \sum_{l,k=0}^{m} \sum_{p,q=0}^{n} \sum_{i=0}^{\min(k,q)} \sum_{j=0}^{\min(l,p)} \frac{(m!)^2 (n!)^2 (-1)^{k+q}}{\sqrt{2^{k+l+p+q}} l!k!} \\
&\times \frac{\overline{\mu}_m^k \overline{\mu}_n^q \left(\overline{\mu}_m^*\right)^l \left(\overline{\mu}_n^*\right)^p}{p!q!(m-l)!(m-k)!(n-p)!(n-q)!} \\
&\times \frac{H_{k-i,l-j}(X,-Y) H_{q-i,p-j}(Y,-X)}{i!j!(k-i)!(l-j)!(q-i)!(p-j)!},
\end{aligned} \tag{32}
$$

where we have defined $\overline{\mu}_m = \beta R_1/\sqrt{T_1}, \overline{\mu}_m^* = \alpha^* R_1/\sqrt{T_1}$, and $\overline{\mu}_n = \beta R_2/\sqrt{T_2}, \overline{\mu}_n^* = \alpha^* R_2/\sqrt{T_2}$ as well as

$$
X = \left(\beta\sqrt{T_2} + \alpha^*\sqrt{T_1}\right)/\sqrt{2}, \tag{33}
$$

$$
Y = \left(\alpha^*\sqrt{T_2} + \beta\sqrt{T_1}\right)/\sqrt{2}, \tag{34}
$$

$$
\begin{aligned}
A = \bar{N}_m^2 \bar{N}_n^2 e^{-\frac{1}{2}(\alpha^*\sqrt{T_2} - \beta\sqrt{T_1})(\beta\sqrt{T_2} - \alpha^*\sqrt{T_1})} \\
\times \left\langle \alpha\sqrt{T_1} \middle| \beta\sqrt{T_1} \right\rangle \left\langle \alpha\sqrt{T_2} \middle| \beta\sqrt{T_2} \right\rangle \\
(\alpha, \beta = z, -z).
\end{aligned} \tag{35}
$$

Here we should point out that $F^{z,z} = F^{-z,-z}, F^{z,-z} = F^{-z,z}$. In particular, when $T_1 = T_2 = 1$ corresponding to the EECSs as entangled channel, from equations (31)–(35) it is ready to get $F(EECS\quad) = [e^{(z^*-z)^2/2} + e^{-4|z|^2 + (z^*+z)^2/2}]/[2(1 + e^{-4|z|^2})]$, which is the fidelity when the EECSs used as the entangled channel [13]. On the other hand, when $m = n = 0$ corresponding to the zero-photon catalysis, from equations (31)–(35) it is also ready to get the fidelity

$$
\begin{aligned}
F_0 = e^{-\frac{1}{2}|z|^2(T_1+T_2) + \frac{1}{2}\left(z^{*2}+z^2\right)\sqrt{T_1 T_2}} \\
\times \left[1 + e^{-|z|^2(T_1+T_2)}\right] \\
/\left\{2\left[1 + e^{-2|z|^2(T_1+T_2)}\right]\right\},
\end{aligned} \tag{36}
$$

which depends on T_1, T_2, and also reduces to $F(EECS)$ for the case of $T_1 = T_2 = 1$, as expected. Thus we can modulate the fidelity by changing T_1 and T_2.

In order to see whether the catalyzed states can be used to realize a teleportation with fidelity over the classical threshold 0.5 [37], we plot the fidelity as the function of coherent amplitude and transmission $T_1 = T_2 = T$ for different values of $m = n$ in figure 10. From figure 10(a), it is shown that for symmetrical transmission case of $T = 0.5$, the fidelity with $m = n = 1$ is less than 0.5 which indicates that the fidelity over 0.5 can not be achieved by single-photon catalysis. As the increasing number of $m = n$ the fidelity increases in a certain small amplitude. Specially, when $m = n \geqslant 3$ the fidelity with the LPE-EECSs as the channel surpasses that with the EECSs as channel in a small amplitude region. It is interesting to note that for zero-photon catalysis of $m = n = 0$ the fidelity can be improved in a large amplitude region compared to the EECSs. Actually, the output state is still an EECSs with a smaller amplitude $z\sqrt{T}$ compared to the initial EECSs, thus the fidelity will be displaced along z axis for a given $T < 1$. These cases are similar to the EPR correlation (see figure 4). Figure 10(b) shows the fidelity as the function of the transmission T for a given $z = 0.5$. It is found that (i) the fidelity first increases then decreases as the increasing T (with $m = n \geqslant 1$) and finally approaches the same value in the limit of $T \to 1$ for different values of $m = n$; (ii) all these maximum values exceed the fidelity with the EECSs channel in a certain region of T, which indicates that the fidelity can be improved by modulating the transmission T. Both the maximum values and the values of T corresponding to these maximum increase as the increasing $m = n$.

Next, we further consider the effects of two different parameters T_1 and T_2 as well as the amplitude z on the fidelity. In figure 11, we plot the fidelity of the LPE-EECSs and the fidelity

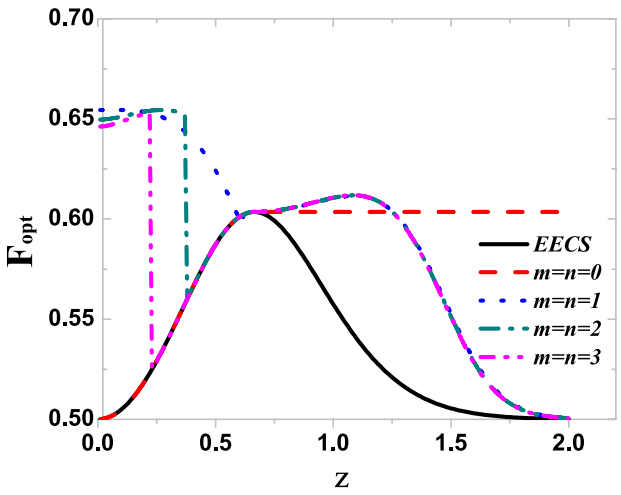

Figure 12. Optimized fidelity of the teleportation (denoted by F_{opt}) when the LPE-EECSs used as entangled resources as a function of the amplitude z for several different photon catalysis cases $m = n = 0, 1, 2, 3$. Here for a comparison, we plot the fidelity of quantum teleportation when the EECSs used as an entangled resource.

difference $\Delta F = F$ (*LPE-EECSs*) $- F$(*EECSs*) by taking the cases of $m = n = 1, 2$ as examples in (T_1, T_2) phase space with $z = 0.5$ and in (z, T) space with $T = T_1 = T_2$, respectively. It is found that (i) there are two regions with $F \geqslant 0.5$ in the phase space both (z, T) and (T_1, T_2) (see the shading regions in figures 11(a)–(d)), but there is only a region with $F \geqslant 0.5$ in high transmission region as the increasing amplitude (see figures 11(a) and (c)); (ii) Compared to the initial EECSs, there are two improved regions of fidelity in low and high transmission, respectively. Moreover, the improved region in low T and high T become bigger and smaller, respectively, as the increasing $m = n$ (see the shading regions in figures 11(e) and (g)). For a given amplitude $z = 0.5$, the improved region moves towards high transmissivity as the increasing $m = n$ (see the shading regions in figures 11(f) and (h)). For a small amplitude, the improved fidelity can be achieved by modulating the transmissivity to a corresponding small value, while for a big amplitude the improvement can be realized in the region of high transmissivity (see the shading regions in figures 11(e) and (g)).

In figure 12, we show the optimal fidelity over T_1 and T_2 as the function of amplitude for different $m = n = 0, 1, 2, 3$. It is clearly seen that (i) for the case of $m = n = 0$, both the LPE-EECSs and the EECSs share the same fidelity within an amplitude range from 0 to 0.66; for a large amplitude ($z > 0.66$), the fidelity for the LPE-EECSs keeps a constant about 0.60, while the fidelity for the EECSs decreases as the increasing amplitude. This indicates that one can keep the maximum fidelity by modulating transmissivity for different amplitude, i.e. the amplitude $z\sqrt{T}$ can be modulated to equal 0.66, which corresponds to the maximum fidelity for the EECSs. (ii) The enhanced region of optimal fidelity for the LPE-EECSs decreases with the increasing photon catalysis number $m = n(= 1, 2, 3)$ in a small amplitude range ($z < 0.66$), which is different from the enhanced concurrence where the maximum entanglement are shared by $m = n(= 1, 2, 3)$. Specially speaking, the regions are about $z < 0.66$, $z < 0.38$ and $z < 0.23$, for $m = n = 1, 2, 3$, respectively. However, for a large amplitude range ($z > 0.66$), different LPE-EECSs with $m = n \neq 0$ share a same enhanced fidelity compared to the EECSs. In addition, it is interesting to notice that for the amplitude range about $0.66 < z < 1.25$, the improvement of the fidelity for $m = n = 1, 2, 3$ performs better than that for $m = n = 0$; While for the amplitude range $z > 1.25$, the latter is always better than the former for the fidelity improvement. These results show that two single-photon catalysis shows the best performance for improving fidelity in the region of $0.38 < z < 1.25$, while zero-photon catalysis presents the best performance in the region of $z > 1.25$. It will be interesting to note the similarity between the optimal fidelity in figure 12 and the optimal EPR correlation in figure 5, which may imply that the EPR enhancement will definitely lead to the fidelity enhancement. Actually, figures 5 and 12 are similar except that the z-values for the peaks are different. The reason can be clearly seen by examining the cases of the initial EECSs that the z-values of 0.56 and 0.66 correspond to the valley and peak of the EPR correlation and the fidelity, respectively.

5. Conclusions

In summary, we propose a scheme, i.e. by introducing the multiphoton catalysis consisting of two beam splitters and conditional measurement on two-mode EECSs for improving the degree of entanglement. It is shown that the output state can be considered as a kind of Laguerre polynomial excited EECSs where the EECSs are characteristic of a smaller coherent amplitude compared to the input EECSs. Its normalization factor is related to two variable Hermite polynomials. It is interesting to note that for zero-photon catalysis, the output states are still EECSs with a smaller amplitude. This indicates that the zero-photon catalysis can be seen as noiseless attenuation process.

According to the EPR correlation and the concurrence, we further investigated the entanglement properties of the LPE-EECSs. Under symmetrical beam splitters case ($T_1 = T_2 = 0.5$), the EPR correlation and the concurrence can only be improved by multi-photon catalysis ($m = n \geqslant 3$), and the corresponding values increase as the increasing catalysis photon number. However, it is interesting that the EPR correlation can be enhanced by zero-photon catalysis. Then we considered the optimal EPR correlation and the concurrence over different T_1 and T_2, respectively. It is shown that for the concurrence, the maximum optimal concurrence (unit) is shared by all non-zero photon catalysis. The optimal value of concurrence corresponding to zero-photon catalysis equals that of the initial EECSs, which is different from the EPR correlation case. For the EPR correlation, however, the optimal results show that (i) one can obtain the EPR minimum values by choosing T_1 and T_2 when the amplitude exceeds a certain threshold (about 0.56) for $m = n = 0$; (ii) the case with $m = n = 1$ presents the best performance for improving the EPR correlation within a certain region (about

$0.27 \sim 1.06$), while the case of $m = n = 0$ shows the best performance when exceeding the value 1.06. In other words, two single-photon catalysis and zero-photon catalysis is the best for improving the EPR correlation in small and large amplitude regions, respectively. In addition, for a small amplitude range, the enhanced region of the EPR correlation decreases with increasing the photon catalysis $m = n = 1, 2, 3$.

Finally, we examined the performance of teleporting unknown coherent state by using the LPE-EECSs as the entangled resource. These optimized results show that (i) the zero-photon catalysis can be used to enhance the fidelity in the region of $z > 0.66$ and the fidelity equals a constant (about 0.60); (ii) The enhanced region of optimal fidelity decreases with the increasing photon catalysis number in a small amplitude range ($z < 0.66$). For a large amplitude range ($z > 0.66$), different LPE-EECSs share a same enhanced fidelity, and the improvement for $m = n \neq 0$ is better than that for $m = n = 0$ within $0.66 < z < 1.25$. The opposite is true for the amplitude range $z > 1.25$. These results are similar to those of EPR correlation. Two single-photon catalysis and zero photon catalysis have a better performance within a small and large amplitude region, respectively, for both the EPR correlation and the fidelity.

Acknowledgments

This work was supported by the National Nature Science Foundation of China (Grant Nos. 11664017 and 11464018) and the Outstanding Young Talent Program of Jiangxi Province (No. 20171BCB23034) as well as the the Natural Science Foundation of Jiangxi Province of China (Grant Nos. 20151BAB212006 and 20142BAB212004), the Research Foundation of the Education Department of Jiangxi Province of China (Nos. GJJ14274 and GJJ14275), together with the Degree and Postgraduate Education Teaching Reform Project of Jiangxi Province (No. JXYJG-2013-027).

References

[1] Bouwmeester D, Ekert A and Zeilinger A 2000 *The Physics of Quantum Information* (Berlin: Springer)
[2] Cerf N J, Leuchs G and Polzik E S (ed) 2007 *Quantum Information with Continuous Variables of Atoms and Light* (London: Imperial College Press)
[3] Nielsen M A and Chuang I L 2000 *Quantum Computation and Quantum Information* (Cambridge: Cambridge University Press)
[4] Eisert J, Scheel S and Plenio M B 2002 Distilling Gaussian states with Gaussian operations is impossible *Phys. Rev. Lett.* **89** 137903
[5] Lee S Y, Ji S W, Kim H J and Nha H 2011 Enhancing quantum entanglement for continuous variables by a coherent superposition of photon subtraction and addition *Phys. Rev.* A **84** 012302
[6] Lee S Y and Nha H 2010 Quantum state engineering by a coherent superposition of photon subtraction and addition *Phys. Rev.* A **82** 053812
[7] Kitagawa A, Takeoka M, Sasaki M and Chefles A 2006 Entanglement evaluation of non-Gaussian states generated by photon sub-traction from squeezed states *Phys. Rev.* A **73** 042310
[8] Benlloch C N, Patron R G, Shapiro J H and Cerf N J 2012 Enhancing quantum entanglement by photon addition and subtraction *Phys. Rev.* A **86** 012328
[9] Bartley T J, Crowley P J D, Datta A, Nunn J, Zhang L J and Walmsley I 2013 Strategies for enhancing quantum entanglement by local photon subtraction *Phys. Rev.* A **87** 022313
[10] Yang Y and Li F L 2009 Entanglement properties of non-Gaussian resources generated via photon subtraction and addition and continuous-variable quantum-teleportation improvement *Phys. Rev.* A **80** 022315
[11] Ourjoumtsev A, Dantan A, Brouri R T and Grangier P 2007 Increasing entanglement between Gaussian states by coherent photon subtraction *Phys. Rev. Lett.* **98** 030502
[12] Opatrny G, Kurizki T and Welsch D-G 2000 Improvement on teleportation of continuous variables by photon subtraction via conditional measurement *Phys. Rev.* A **61** 032302
[13] Wu J N, Liu S Y, Hu L Y, Huang J H, Duan Z L and Ji Y H 2015 Improving entanglement of even entangled coherent states by a coherent superposition of photon subtraction and addition *J. Opt. Soc. Am.* B **32** 2299
[14] Kurochkin Y, Prasad A S and Lvovsky A I 2014 Distillation of the two-mode squeezed state *Phys. Rev. Lett.* **112** 070402
[15] Kim H J, Kim J and Nha H 2013 Enhanced multipartite quantum correlation by non-Gaussian operations *Phys. Rev.* A **88** 032109
[16] Su Y C and Wu S T 2017 Entanglement enhancement through multirail noise reduction for continuous-variable measurement-based quantum-information processing *Phys. Rev.* A **96** 032327
[17] Ren G, Du J M, Yu H J and Xu Y J 2012 Nonclassical properties of Hermite polynomial's coherent state *J. Opt. Soc. Am.* B **29** 3412
[18] Liu S Y, Li Y Z, Hu L Y, Huang J H, Xu X X and Tao X Y 2015 Nonclassical properties of Hermite polynomial excitation on squeezed vacuum and its decoherence in phase-sensitive reservoirs *Laser Phys. Lett.* **12** 045201
[19] Ye W, Zhou W D, Zhang H L, Liu C J, Huang J H and Hu L Y 2017 Laguerre polynomial excited coherent state: generation and nonclassical properties *Laser Phys. Lett.* **14** 115201
[20] Liu C J, Ye W, Zhou W D, Zhang H L, Huang J H and Hu L Y 2017 Entanglement of coherent superposition of photon-subtraction squeezed vacuum *Front. Phys.* **12** 120307
[21] Lundeen J S, Feito A, Coldenstrodt-Ronge H, Pregnell K L, Silberhorn Ch, Ralph T C, Eisert J, Plenio M B and Walmsley I A 2009 Tomography of quantum detectors *Nat. Phys.* **5** 27–30
[22] Zavatta A, Fiurasek J and Bellini M 2011 A high-fidelity noiseless amplifier for quantum light states *Nat. Photon.* **5** 52–60
[23] Guo Y, Liao Q, Wang Y J, Huang D, Huang P and Zeng G H 2017 Performance improvement of continuous-variable quantum key distribution with an entangled source in the middle via photon subtraction *Phys. Rev.* A **95** 032304
[24] Zhou N R, Li J F, Yu Z B, Gong L H and Farouk A 2017 New quantum dialogue protocol based on continuous-variable two-mode squeezed vacuum states *Quantum Inf. Process.* **16** 4
[25] Gong L H, Song H C, He C S, Liu Y and Zhou N R 2011 A continuous variable quantum deterministic key distribution based on two-mode squeezed states *Phys. Scr.* **89** 035101
[26] van Enk S J and Hirota O 2001 Entangled coherent states: teleportation and decoherence *Phys. Rev.* A **64** 022313
[27] Joo J, Munro W J and Spiller T P 2011 Quantum metrology with entangled coherent states *Phys. Rev. Lett.* **107** 083601

[28] Joo J, Munro W J and Spiller T P 2011 Quantum metrology with entangled coherent states (*Phys. Rev. Lett.* 107 083601) *Phys. Rev. Lett.* **107** 219902 (erratum)
[29] Zhang Z J, Qiao T Y, Song J, Cen L Z, Zhang J D, Li S, Yan L Y, Wang F and Zhao Y 2017 Improved resolution and sensitivity of angular rotation measurement using entangled coherent states *Opt. Commun.* **403** 92–6
[30] Zhang Y M, Li X W, Yang W and Jin G R 2013 Quantum Fisher information of entangled coherent states in the presence of photon loss *Phys. Rev.* A **88** 043832
[31] An N B 2004 Optimal processing of quantum information via W-type entangled coherent states *Phys. Rev.* A **69** 022315
[32] Sangouard N, Simon C, Gisin N, Laurat J, Brouri R T and Grangier P 2010 Quantum repeaters with entangled coherent states *J. Opt. Soc. Am.* B **27** 137–45
[33] Munro W J, Milburn G J and Sanders B C 2000 Entangled coherent-state qubits in an ion trap *Phys. Rev.* A **62** 052108
[34] Wang X G 2001 Quantum teleportation of entangled coherent states *Phys. Rev.* A **64** 022302
[35] Sanders B C 2012 Review of entangled coherent states *J. Phys. A: Math. Theor.* **45** 244002
[36] Hu L Y and Fan H Y 2009 Multipartite coherent entangled state of continuous variables: structure and generation *Int. J. Mod. Phys.* A **24** 2689–701
[37] Zhang H L, Jia F, Xu X X, Tao X Y and Hu L Y 2012 Nonclassicality and decoherence of photon-subtraction squeezing-enhanced thermal state *Int. J. Theor. Phys.* **51** 3330–43
[38] Wang D, Li M, Zhu F, Yin Z Q, Chen W, Han Z F, Guo G C and Wang Q 2014 Quantum key distribution with the single-photon-added coherent source *Phys. Rev.* A **90** 062315
[39] Lvovsky A I and Mlynek J 2002 Quantum-optical catalysis: generating nonclassical states of light by means of linear optics *Phys. Rev. Lett.* **88** 250401
[40] Hu L Y, Wu J N, Liao Z Y and Zubairy M S 2016 Multiphoton catalysis with coherent state input: nonclassicality and decoherence *J. Phys. B: At. Mol. Opt. Phys.* **49** 175504
[41] Hu L Y, Liao Z Y and Zubairy M S 2017 Continuous-variable entanglement via multiphoton catalysis *Phys. Rev.* A **95** 012310
[42] Ulanov A E, Fedorov I A, Pushkina A A, Kurochkin Y V, Ralph T C and Lvovsky A I 2015 Undoing the effect of loss on quantum entanglement *Nat. Photon.* **9** 764–8
[43] Hu L Y, Liao Z Y, Ma S L and Zubairy M S 2016 Optimal fidelity of teleportation with continuous variables using three tunable parameters in a realistic environment *Phys. Rev.* A **93** 033807
[44] Jia F, Xu X X, Liu C J, Huang J H, Hu L Y and Fan H Y 2014 Decompositions of beam splitter operator and its entanglement function *Acta Phys. Sin.* **63** 220301
[45] Zheng K M, Liu S Y, Zhang H L, Liu C J and Hu L Y 2014 A generalized two-mode entangled state: its generation, properties, and applications *Front. Phys.* **9** 451–9
[46] Jeong H, Kim M S and Lee J 2001 Quantum-information processing for a coherent superposition state via a mixed entangled coherent channel *Phys. Rev.* A **64** 052308
[47] Duan L M, Giedke G, Cirac J I and Zoller P 2000 Inseparability criterion for continuous variable systems *Phys. Rev. Lett.* **84** 2722
[48] Mann A, Sanders B C and Munro W J 1995 Bell's inequality for an entanglement of nonorthogonal states *Phys. Rev.* A **51** 989
[49] Hill S and Wootters W K 1997 Entanglement of a pair of quantum bits *Phys. Rev. Lett.* **78** 5022
[50] Wootters W K 1998 Entanglement of formation of an arbitrary state of two qubits *Phys. Rev. Lett.* **80** 2245
[51] Braunstein S L and Kimble H J 1998 Teleportation of continuous quantum variables *Phys. Rev. Lett.* **80** 869
[52] Zubairy M S 1998 Quantum teleportation of a field state *Phys. Rev.* A **58** 4368
[53] Marian P and Marian T A 2006 Continuous-variable teleportation in the characteristic-function description *Phys. Rev.* A **74** 042306